

Safe Feedback Motion Planning: A Contraction Theory and \mathcal{L}_1 -Adaptive Control Based Approach

Arun Lakshmanan[†], Aditya Gahlawat[†], and Naira Hovakimyan

Abstract— Autonomous robots that are capable of operating safely in the presence of imperfect model knowledge or external disturbances are vital in safety-critical applications. In this paper, we present a planner-agnostic framework to design and certify safe tubes around desired trajectories that the robot is always guaranteed to remain inside. By leveraging recent results in contraction analysis and \mathcal{L}_1 -adaptive control we synthesize an architecture that induces safe tubes for nonlinear systems with state and time-varying uncertainties. We demonstrate with a few illustrative examples¹ how contraction theory-based \mathcal{L}_1 -adaptive control can be used in conjunction with traditional motion planning algorithms to obtain provably safe trajectories.

Index Terms— feedback motion planning, robust trajectory tracking, \mathcal{L}_1 -adaptive control, contraction theory, control contraction metrics, robust adaptive control, nonlinear reference s.

I. INTRODUCTION

Motion planning algorithms generate optimal open-loop trajectories for robots to follow; however, any uncertainty in the system can potentially drive the robot far away from the desired path. For instance, quadrotors experience blade-flapping and induced drag forces that are dependent on the velocity, ground effects that are dependent on the altitude, and external wind effects that are often unaccounted for by the motion planner, [2]. Accurate modeling of these uncertainty effects on system dynamics can be very expensive and time-consuming. A widely accepted approach to account for uncertainty in motion planning is through feedback [3, Chapter 8]. In practice, ancillary tracking controllers or model predictive control (MPC) schemes are employed to alleviate this problem. However, the presence of the uncertainties is not explicitly considered in the control design process, and instead the performance is achieved with hand-tuned controller parameters and experimental validation. Without valid safety certificates, the uncertainty might drive the system unstable and far enough away from the desired trajectory, resulting in collisions with obstacles, Fig. 1a.

Robust trajectory tracking controllers using classical Lyapunov stability theory have been designed for helicopters [4], hovercraft [5], marine vehicles [6], and several other autonomous robots, which exhibit nonlinear behavior. These

^{*}This work is financially supported by AFOSR, National Aeronautics and Space Administration (NASA) and National Science Foundation's NRI and Cyber Physical Systems (CPS) awards #1830639 and #1932529.

The authors are with the Department of Mechanical Science and Engineering, University of Illinois at Urbana-Champaign, Urbana, IL 61801, USA (e-mail: {lakshma2, gahlawat, nhovakim}@illinois.edu).

[†]These authors contributed equally to this work.

¹Due to space limitations the examples are included in the extended version of this paper [1].

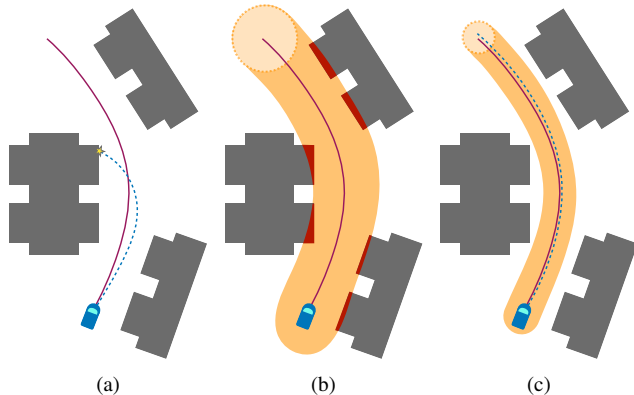


Fig. 1. Although the planned path is collision free (purple), the robot's actual trajectory (dashed-blue) might lead to a collision with the obstacles (gray) in the environment due to model discrepancies or external disturbances. (b) A feedback policy ensures that the robot stays inside of the (orange) tube which is too wide to pass between the obstacles without colliding (c) The safe feedback controller proposed in this paper guarantees that the robot's trajectory never escapes the tube, which itself is also collision-free.

approaches rely on backstepping techniques, sliding-mode control, passivity-based control, or other robust nonlinear control design tools [7, Chapter 14]. However, the classical methods do not provide a ‘one size fits all’ procedure for the constructive design of tracking controllers for a large class of nonlinear systems. Unless the problem has a very specific structure that can be exploited, a control Lyapunov function (CLF) has to be found which can be prohibitively difficult for general nonlinear systems because the feasibility conditions do not appear as linear matrix inequalities (LMI), unlike in case of linear systems.

Advances in computational resources and optimization toolboxes available to autonomous robots have led to active developments in the field of robust MPC. The two large classes of methods of interest are min-max MPC [8], [9], [10] and tube-based MPC [11], [12], [13], [14], [15]. Min-max MPC approaches consider the worst-case disturbance that can affect the system making them overly conservative. If the uncertainty is too large or the robot is planning over a long horizon, a min-max MPC based approach may even render the optimization infeasible. Tube-based MPC methods address these issues by employing an ancillary controller to attenuate disturbances and ensure that the robot stays inside of a ‘tube’ around the desired trajectory. However, with the exception of [15], these methods assume the existence of a stabilizing ancillary controller and its region of attraction

along the desired trajectory. Moreover, the resulting tubes are of fixed width, which may be overly conservative depending on the operating conditions (see Fig. 1b). This issue is partly addressed for feedback linearizable systems in [15] by using sliding-mode boundary layer control to construct tubes of any desired size during the MPC optimization procedure. Furthermore, unlike classical methods, the MPC-based approaches while applicable to larger class of systems incur a heavy computational load and are not always amenable to real-time applications.

Contraction theory-based approaches [16], [17] bridge the gap between classical and optimization-based methods, and provide a constructive control design procedure for nonlinear systems. In [18], the authors introduce contraction analysis as a tool for studying stability of nonlinear systems using differential geometry. In particular, the authors show that the ‘contracting’ or convergent nature of solutions to nonlinear systems can be derived from the differential dynamics of the system. Since the differential dynamics for nonlinear systems are of linear-time varying (LTV) form, all the results from linear systems theory can be leveraged for nonlinear systems through the contraction analysis framework. In [16], constructive control design techniques from linear systems theory can be used to find a control contraction metric (CCM), which is analogous to CLFs in the differential framework. This is significantly easier than directly finding the CLFs for nonlinear systems, because the feasibility conditions for CCMs are represented as LMIs. In [19], a design procedure for synthesizing CCM-based controllers is given, which induces fixed-width tubes in the presence of bounded external disturbances, excluding modeling uncertainties. However, as discussed before, fixed-width tubes might result in infeasibility of the problem and result in more work for the planner to find a more conservative path that produces feasible tubes. More recently, in [20] a model reference control architecture in conjunction with CCM-based feedback is proposed for handling uncertainties in the system.

In this paper, we present an approach for safe feedback motion planning for control-affine nonlinear systems that relies on contraction theory-based solution for exponential stabilizability around trajectories and \mathcal{L}_1 -adaptive control for handling uncertainties and providing guarantees for transient performance and robustness. In \mathcal{L}_1 control architecture, estimation is decoupled from control, thereby allowing for arbitrarily fast adaptation subject only to hardware limitations, [21]. The \mathcal{L}_1 control has been successfully implemented on NASA’s AirStar 5.5% subscale generic transport aircraft model [22], Calspan’s Learjet [23], and unmanned aerial vehicles [24], [25]. In [26], the authors presented the analysis for the \mathcal{L}_1 -adaptive control architecture with nonlinear time-varying reference systems. However, the stabilizability of the nominal nonlinear model and associated safety certificates were simply assumed. In this paper, we present a constructive design of feedback strategy for nonlinear systems using CCMs and \mathcal{L}_1 -adaptive control that provides strong guarantees of transient performance and robustness for a large

class of control-affine nonlinear systems. Furthermore, we show how this control architecture induces tubes that can be flexibly changed to ensure safety based on the uncertainty in the system and the environment. In particular, this flexibility is provided by the architecture of the \mathcal{L}_1 -adaptive control by decoupling the control loop from the estimation loop [21]. In this way, the width of the certifiable tubes can be adjusted allowing the safe operation of a robot in tight confines.

The manuscript is organized as follows. The problem statement and the assumptions are provided in Section II. The proposed controller is presented in Section III and the stability analysis of the closed-loop system is provided in Section IV. Due to space limitations the description of the notations, preliminaries, simulation examples, and proofs have been moved to the extended version of this paper [1].

II. PROBLEM STATEMENT

We consider systems for which the evolution of dynamics can be represented as

$$\dot{x}(t) = F(x(t), u(t)) \quad (1a)$$

$$= f(x(t)) + B(x(t))(u(t) + h(t, x(t))), \quad (1b)$$

with initial condition $x(0) = x_0$, where $x(t) \in \mathbb{R}^n$ is the system state and $u(t) \in \mathbb{R}^m$ is the control input. The functions $f(x) \in \mathbb{R}^n$ and $B(x) \in \mathbb{R}^{n \times m}$ are known, and $h(t, x) \in \mathbb{R}^m$ represents the uncertainties. The *nominal dynamics* ($h \equiv 0$) are therefore represented as

$$\dot{x}(t) = \bar{F}(x(t), u(t)) \quad (2a)$$

$$= f(x(t)) + B(x(t))u(t), \quad x(0) = x_0. \quad (2b)$$

Consider a *desired control trajectory* $u^*(t) \in \mathbb{R}^m$ and the induced *desired state trajectory* $x^*(t) \in \mathbb{R}^n$ from any planner based on nominal dynamics

$$\dot{x}^*(t) = \bar{F}(x^*(t), u^*(t)), \quad x^*(0) = x_0^*. \quad (3)$$

Together, $(x^*(t), u^*(t))$ is referred to as the *desired state-input trajectory pair*. The planner ensures that the desired state-trajectory $x^*(t)$ remains in a compact *safe set* $\mathcal{X} \subset \mathbb{R}^n$, for all $t \geq 0$.

The goal is to design a control input $u(t)$ so that the state $x(t)$ of the uncertain system in (1) remains ‘close’ to the desired trajectory $x^*(t)$ while also ensuring $x(t) \in \mathcal{X}$, for all $t \geq 0$. In order to rigorously define the notion of ‘closeness’, we need the following definition:

Definition 2.1: Given a positive scalar ρ and the desired state trajectory $x^*(t)$, $\Omega(\rho, x^*(t))$ denotes the ρ -norm ball around $x^*(t)$, i.e.

$$\Omega(\rho, x^*(t)) := \{y \in \mathbb{R}^n \mid \|y - x^*(t)\| \leq \rho\}. \quad (4)$$

Clearly $\Omega(\rho, x^*(t))$ induces a *tube* centered around $x^*(t)$, where the tube is given by

$$\mathcal{O}(\rho) := \bigcup_{t \geq 0} \Omega(\rho, x^*(t)), \quad (5)$$

with $\rho > 0$ as the radius.

The problem under consideration can now be stated as follows: given the desired trajectory $x^*(t) \in \mathcal{X}$ and a positive scalar ρ , design a control input $u(t)$ such that the state of the uncertain system (1) satisfies:

$$x(t) \in \Omega(\rho, x^*(t)) \subset \mathcal{X}, \quad \forall t \geq 0.$$

Note the condition that $\Omega(\rho, x^*(t)) \subset \mathcal{X}$ is dependent on the desired trajectory $x^*(t)$ (given by the planner) and the tube width ρ (chosen by the user). To ensure that this control-independent condition is satisfied, we place the following assumption.

Assumption 2.1: Given the positive scalar ρ , the desired state trajectory satisfies $x^*(t) \in \mathcal{X}_\rho$, for all $t \geq 0$, where

$$\mathcal{X}_\rho = \mathcal{X} \ominus \mathcal{B}(\rho), \quad \mathcal{B}(\rho) := \{y \in \mathbb{R}^n \mid \|y\| \leq \rho\}, \quad (6)$$

and the desired control input $u^*(t)$ is bounded for all $t \geq 0$.

Remark 2.1: The implication of Assumption 2.1 is that if the state trajectory satisfies $x(t) - x^*(t) \in \mathcal{B}(\rho)$ and $x^*(t) \in \mathcal{X}_\rho$, for all $t \geq 0$, then the definition of the Pontryagin set difference [27, Chapter 3] implies that $x(t) \in \Omega(\rho, x^*(t)) \subset \mathcal{X}$, for all $t \geq 0$.

Next, we place assumptions on the boundedness and continuity properties of the system functions and uncertainties.

Assumption 2.2: The functions $f(x) \in \mathbb{R}^n$, $B(x) \in \mathbb{R}^{n \times m}$, and $h(t, x) \in \mathbb{R}^m$ are continuous, bounded, and Lipschitz in x , uniformly in t , for all $x \in \mathcal{X}$ and $t \geq 0$. Moreover, $B(x)$ has full column rank for all $x \in \mathcal{X}$.

Assumption 2.3: The derivatives $\frac{\partial f}{\partial x}(x)$, $\frac{\partial B}{\partial x}(x)$, $\frac{\partial h}{\partial x}(t, x)$, and $\frac{\partial h}{\partial t}(t, x)$ are bounded for all $x \in \mathcal{X}$ and $t \geq 0$.

Given any $\rho > 0$, based on Assumptions 2.1 to 2.3, we have that for all $x \in \mathcal{O}(\rho)$ and $t \geq 0$ the following hold

$$\|u^*\| \leq \Delta_{u^*}, \quad \|f\| \leq \Delta_f, \quad \left\| \frac{\partial f}{\partial x} \right\| \leq \Delta_{f_x}, \quad (7a)$$

$$\|B\| \leq \Delta_B, \quad \sum_{i=1}^n \left\| \frac{\partial B}{\partial x} \right\| \leq \Delta_{B_x}, \quad \sum_{j=1}^m \left\| \frac{\partial b_j}{\partial x} \right\| \leq \Delta_{b_x}, \quad (7b)$$

$$\|B^\dagger\| \leq \Delta_{B^\dagger}, \quad \sum_{i=1}^n \left\| \frac{\partial B^\dagger}{\partial x_i} \right\| \leq \Delta_{B_x^\dagger}, \quad (7c)$$

$$\|h\| \leq \Delta_h, \quad \left\| \frac{\partial h}{\partial x} \right\| \leq \Delta_{h_x}, \quad \left\| \frac{\partial h}{\partial t} \right\| \leq \Delta_{h_t}, \quad (7d)$$

where the function arguments are omitted for brevity, b_j denotes the j^{th} column of $B(x)$, $B^\dagger(x) = (B^\top(x)B(x))^{-1}B^\top(x)$ denotes the Moore-Penrose inverse, which is guaranteed to exist by Assumption 2.2.

Contraction theory allows to synthesize feedback laws so that, in the absence of uncertainties, the state of the nominal dynamics in (2) tracks a feasible desired trajectory $x^*(t)$. A more detailed introduction to contraction theory is available in [1, Sec. 3]. We place the following assumption on the nominal dynamics.

Assumption 2.4: The nominal dynamics in Eq. (2) admit a control contraction metric $M(x)$ for all $x \in \mathcal{X}$ with positive scalars λ , $\underline{\alpha}$, and $\bar{\alpha}$, as in [1, Definition 3.1].

III. CONTRACTION THEORY BASED \mathcal{L}_1 -ADAPTIVE CONTROL

In this section we introduce the structure of the proposed controller for the uncertain nonlinear system in Eq. (1). Consider the following feedback decomposition

$$u(t) = u_c(t) + u_a(t), \quad (8)$$

where $u_c : \mathbb{R}_{\geq 0} \rightarrow \mathbb{R}^m$ is the contraction theory based control designed to guarantee universal exponential stability (UES) of the nominal dynamics in Eq. (2), and $u_a : \mathbb{R}_{\geq 0} \rightarrow \mathbb{R}^m$ is the \mathcal{L}_1 control signal. The overall architecture of the proposed feedback is illustrated in Fig. 2. We refer to the uncertain system in Eq. (1) with the feedback law Eq. (8) as the \mathcal{L}_1 closed-loop system. Before we proceed with the description of the individual components of the controller, we introduce the following list of constants that are of importance for the results presented in this paper:

$$\Delta_{M_x} := \sup_{x \in \mathcal{O}(\rho)} \sum_{i=1}^n \left\| \frac{\partial M}{\partial x_i}(x) \right\|, \quad (9)$$

$$\Delta_{\Psi_x} := 2\Delta_{B_x} + \frac{\Delta_B \Delta_{M_x}}{\underline{\alpha}}, \quad (10)$$

$$\Delta_{\delta_u} := \frac{1}{2} \sup_{x \in \mathcal{O}(\rho)} \left(\frac{\bar{\lambda}(L^{-\top}(x)F(x)L^{-1}(x))}{\underline{\sigma}_{>0}(B^\top(x)L^{-1}(x))} \right), \quad (11)$$

$$\Delta_{\dot{x}_r} := \Delta_f + \Delta_B (\|\mathbb{I}_m - C(s)\|_{\mathcal{L}_1} \Delta_h + \Delta_{u^*} + \rho \Delta_{\delta_u}), \quad (12)$$

$$\Delta_{\dot{x}} := \Delta_f + \Delta_B (2\Delta_h + \Delta_{u^*} + \rho \Delta_{\delta_u}), \quad (13)$$

$$\Delta_{\tilde{x}} := \sqrt{\frac{4\bar{\lambda}(P)\Delta_h(\Delta_{h_t} + \Delta_{h_x}\Delta_{\dot{x}})}{\underline{\lambda}(P)\underline{\lambda}(Q)} + \frac{4\Delta_h^2}{\underline{\lambda}(P)}}, \quad (14)$$

$$\Delta_{\tilde{\eta}} := \left(\Delta_{B_x^\dagger} \Delta_{\dot{x}} + (\|sC(s)\|_{\mathcal{L}_1} + \|A_m\|) \Delta_{B^\dagger} \right) \Delta_{\tilde{x}}, \quad (15)$$

$$\Delta_\theta := \frac{\Delta_B \bar{\alpha} \Delta_{\tilde{\eta}}}{\lambda}, \quad (16)$$

$$\Delta_{\dot{\Psi}} := \bar{\alpha} \left(\Delta_B \Delta_{\dot{\gamma}_s} + \frac{\Delta_B \Delta_{M_x} \Delta_{\dot{x}}}{\sqrt{\bar{\alpha}}\underline{\alpha}} + \Delta_{B_x} \Delta_{\dot{x}} \right), \quad (17)$$

$$\Delta_{\dot{\gamma}_s} := \sqrt{\frac{\bar{\alpha}}{\underline{\alpha}}} \left(\Delta_{f_x} + (\Delta_h + \Delta_{u^*} + \rho \Delta_{\delta_u}) \Delta_{b_x} + \left(\Delta_{h_x} + \frac{\sqrt{\bar{\alpha}} \Delta_{\delta_u}}{\sqrt{\bar{\alpha}}} \right) \Delta_B \right), \quad (18)$$

where $F(x)$ is defined as

$$F(x) := -\partial_f W(x) + 2 \left[\frac{\partial f}{\partial x}(x) W(x) \right]_{\mathbb{S}} + 2\lambda W(x),$$

and $W(x) = M(x)^{-1}$ is referred to as the dual metric, while $L(x)^\top L(x) = W(x)$.

A. Contraction theory based control: $u_c(t)$

We propose the following law

$$u_c(t) = u^*(t) + k_c(x^*(t), x(t)), \quad (19)$$

where, for the feedback term, we use the law constructed in [16, Sec. IV.A], which is the solution to the following

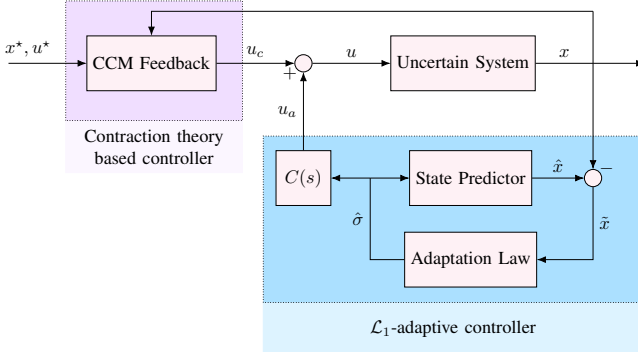


Fig. 2. Architecture of CCM-based \mathcal{L}_1 -adaptive control

quadratic program:

$$k_c(x^*(t), x(t)) = \arg \min_{k \in \mathbb{R}^m} \|k\|^2, \quad (20a)$$

$$\text{s.t. } 2\bar{\gamma}_s^\top(1, t)M(x(t))\dot{x}_k(t) - 2\bar{\gamma}_s^\top(0, t)M(x^*(t))\dot{x}^*(t) \leq -2\lambda\mathcal{E}(x^*(t), x(t)), \quad (20b)$$

with $M(x)$ being the CCM, $\bar{\gamma}(s, t)$, $s \in [0, 1]$, being the minimizing geodesic with $\bar{\gamma}(1, t) = x(t)$ and $\bar{\gamma}(0, t) = x^*(t)$, and $\mathcal{E}(\cdot, \cdot)$ being the Riemannian energy computed along the geodesic. For more details about geodesics and Riemannian energy with regard to contraction theory see [1, Sec. 3]. Additionally, $\dot{x}_k(t) = \bar{F}(x(t), u^*(t) + k)$.

Remark 3.1: As explained by the authors in [19, Sec. 5.1], the solution to the quadratic program in (20) can be obtained analytically given the minimizing geodesic $\bar{\gamma}(\cdot, t)$. Alternatively, one may use the differential controller proposed in [16], albeit at the expense of a larger control effort.

B. \mathcal{L}_1 -adaptive control: $u_a(t)$

The computation of the signal $u_a(t)$ depends on three components illustrated in Fig. 2; namely, the state-predictor, the adaptation law, and a low-pass filter. Similar to [10], we define the *state-predictor* as

$$\dot{x}(t) = \bar{F}(x(t), u_c(t) + u_a(t) + \hat{\sigma}(t)) + A_m \tilde{x}(t), \quad (21)$$

with $\hat{x}(0) = x_0$, and where $\hat{x}(t) \in \mathbb{R}^n$ is the state of the predictor, $\tilde{x}(t) = \hat{x}(t) - x(t)$ is the state prediction error, and $A_m \in \mathbb{R}^{n \times n}$ is an arbitrary Hurwitz matrix.

The *uncertainty estimate* $\hat{\sigma}(t)$ in Eq. (21) is governed by the following *adaptation law*

$$\dot{\hat{\sigma}}(t) = \Gamma \text{Proj}_{\mathcal{H}}(\hat{\sigma}(t), -B(x)^\top P \tilde{x}(t)), \quad \hat{\sigma}(0) \in \mathcal{H}, \quad (22)$$

where $\Gamma > 0$ is the adaptation rate, $\mathcal{H} = \{y \in \mathbb{R}^m \mid \|y\| \leq \Delta_h\}$ is the set in which the uncertainty estimate is restricted to remain in. Furthermore, $\mathbb{S}^n \ni P \succ 0$ is the solution to the Lyapunov equation $A_m^\top P + P A_m = -Q$ for some $\mathbb{S}^n \ni Q \succ 0$. Moreover, $\text{Proj}_{\mathcal{H}}(\cdot, \cdot)$ is the projection operator standard in adaptive control literature [28], [29].

Finally, the control law $u_a(t)$ is defined as the following Laplace transform

$$u_a(s) = -C(s)\hat{\sigma}(s), \quad (23)$$

where $C(s)$ is a low-pass filter with bandwidth ω and satisfies $C(0) = \mathbb{I}_m$. Note that there is an abuse of notation when we denote both the geodesic interval parameter and the Laplace variable by s . The delineation between the two is clear from the context.

C. Filter bandwidth and adaptation rate

The design of the \mathcal{L}_1 -adaptive controller involves the design of a strictly proper and stable low-pass filter $C(s)$ with $C(0) = \mathbb{I}_m$. Let the bandwidth of this filter be ω . In the manuscript, for the sake of simplicity, we choose $C(s) = \frac{\omega}{s+\omega}\mathbb{I}_m$. As we will see in Section IV, the bandwidth ω of the low-pass filter $C(s)$ in Eq. (23) and the adaptation rate Γ in Eq. (22) are tunable parameters. However, these entities need to satisfy a few conditions mentioned below. The reasoning behind these conditions will be made clear in the subsequent section.

Suppose that Assumption 2.4 holds. Then, for arbitrarily chosen positive scalars ϵ and ρ_a , define

$$\rho_r = \sqrt{\frac{\bar{\alpha}}{\underline{\alpha}}}\|x_0^* - x_0\| + \epsilon, \quad (24)$$

$$\rho = \rho_r + \rho_a. \quad (25)$$

Furthermore, suppose that Assumptions 2.1 to 2.3 hold. Define

$$\zeta_1(\omega) = 2\rho\Delta_B \frac{\bar{\alpha}}{\underline{\alpha}} \left(\frac{\Delta_h}{|2\lambda - \omega|} + \frac{\Delta_{h_t} + \Delta_{h_x}\Delta_{\dot{x}_r}}{2\lambda\omega} \right), \quad (26a)$$

$$\zeta_2(\omega) = \bar{\alpha}\Delta_{\dot{x}_r} \left(\frac{\Delta_h}{|2\lambda - \omega|} + \frac{\Delta_{h_t} + \Delta_{h_x}\Delta_{\dot{x}_r}}{2\lambda\omega} \right), \quad (26b)$$

$$\zeta_3(\omega) = \bar{\alpha}\Delta_{h_x} \left(\frac{4\lambda\Delta_B + \Delta_{\dot{\Psi}}}{\lambda\omega} \right), \quad (26c)$$

where $\Delta_{\dot{x}_r}$, $\Delta_{\dot{x}_r}$, and $\Delta_{\dot{\Psi}}$, are known positive scalars defined in Eqs. (10), (12) and (17) respectively. Then, the bandwidth ω of the low-pass filter $C(s)$ and the adaptation rate need to verify the following conditions

$$\rho_r^2 \geq \frac{\mathcal{E}(x_0^*, x_0)}{\underline{\alpha}} + \zeta_1(\omega), \quad (27a)$$

$$\underline{\alpha} > \zeta_2(\omega) + \zeta_3(\omega), \quad (27b)$$

$$\sqrt{\Gamma} > \frac{\Delta_\theta}{\rho_a(\underline{\alpha} - \zeta_2(\omega) - \zeta_3(\omega))}, \quad (27c)$$

where Δ_θ is another known positive scalar defined in Eq. (16).

Remark 3.2: Based on the definition of ρ_r in Eq. (25) and the bounds on the Riemannian energy $\mathcal{E}(x^*(t), x(t))$ as described in [1, Sec. 3], the inequality $\rho_r^2 > \mathcal{E}(x_0^*, x_0)/\underline{\alpha}$ holds. Furthermore, since $\zeta_1(\omega)$, $\zeta_2(\omega)$, and $\zeta_3(\omega)$, all converge to zero as ω increases, the bandwidth conditions in (27a)-(27b) can always be satisfied by choosing a large enough ω .

IV. PERFORMANCE ANALYSIS

In this section we analyze the performance of the uncertain system in Eq. (1) with the \mathcal{L}_1 control feedback $u(t)$ defined in Eq. (8). As in [10], to derive the bounds between the desired trajectory $x^*(t)$ and the state $x(t)$ of the uncertain

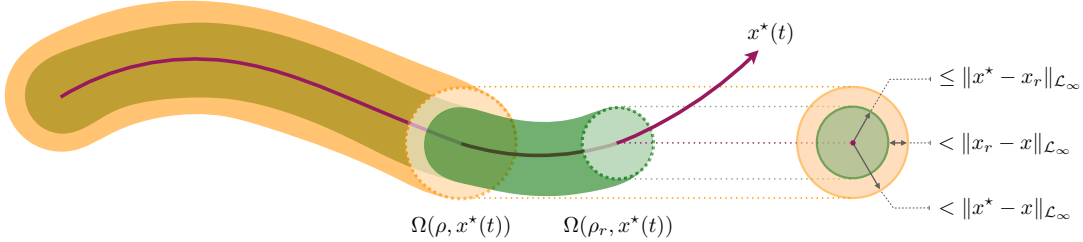


Fig. 3. The performance bounds/tubes for the analysis of the CCM based \mathcal{L}_1 -adaptive controller.

system, we first introduce the following intermediate system, which we refer to as the *reference system*:

$$\begin{aligned}\dot{x}_r(t) &= F(x_r(t), -\eta_r(t)) \\ &= f(x_r(t)) + B(x_r(t))(u_{c,r}(t) - \eta_r(t) + h(t, x_r(t))),\end{aligned}\quad (28a)$$

$$u_{c,r}(t) = u^*(t) + k_c(x^*(t), x_r(t)), \quad (28b)$$

$$\eta_r(s) = C(s)\mathcal{L}[h(t, x_r(t))], \quad x_r(0) = x_0, \quad (28c)$$

where k_c is defined in Eq. (20) using x_r in place of x . The main feature of the reference system is that it defines *the best achievable performance*, given the perfect knowledge of uncertainty, i.e. it reflects that the cancellation of the uncertainty $h(t, x_r(t))$ can happen only within the bandwidth of the low-pass filter.

The analysis consists of two parts: we first derive bounds between the desired trajectory and the reference system $\|x^*(t) - x_r(t)\|$. Then we derive the bounds between the states of the reference system and the actual system $\|x_r(t) - x(t)\|$. Recall that we refer to the actual system as the \mathcal{L}_1 closed loop system, which is given by Eq. (1) with the control law in Eq. (8). Finally, the triangle inequality produces the desired bound on $\|x^*(t) - x(t)\|$. In this way, the reference system behaves as an ‘anchor system’ for the analysis. These bounds are illustrated in Fig. 3. Furthermore, we provide the justification of treating the bandwidth ω of $C(s)$ and the adaptation rate Γ as tuning-knobs. Indeed, the upcoming analysis will show that we can ensure that $x(t) \in \Omega(\rho, x^*(t))$ (see Eq. (4)) for all $t \geq 0$.

We begin with the bound between the reference system state and desired state trajectory. This corresponds to the green tube in Fig. 3. The proofs for all the claims in this section are provided in [1, Appendix B].

Lemma 4.1: Let all the assumptions hold and let ρ_r be as defined in Eq. (25). If the conditions in (27a)-(27b) hold, then for any desired state trajectory $x^*(t)$ the state $x_r(t)$ of the reference system in (28) satisfies

$$x_r(t) \in \Omega(\rho_r, x^*(t)), \quad \forall t \geq 0, \quad (29)$$

and is uniformly ultimately bounded as

$$x_r(t) \in \Omega(\mu(\omega, T), x^*(t)) \subset \Omega(\rho_r, x^*(t)), \quad \forall t \geq T > 0, \quad (30)$$

where the ultimate bound is defined as

$$\mu(\omega, T) := \sqrt{\frac{e^{-2\lambda T} \mathcal{E}(x_0^*, x_0)}{\underline{\alpha}} + \zeta_1(\omega)}. \quad (31)$$

Next, we compute the bounds between the reference system in Eq. (28) and the \mathcal{L}_1 closed-loop system (Eq. (1) with Eq. (8)).

Lemma 4.2: Suppose that the stated assumptions and the conditions in Eq. (27) hold. Additionally, assume that the trajectory of the \mathcal{L}_1 closed-loop system satisfies $x(t) \in \Omega(\rho, x^*(t))$, for all $t \in [0, \tau]$, for some $\tau > 0$, with $\Omega(\rho, x^*(t))$ and ρ defined in Eq. (4) and Eq. (25), respectively. Then,

$$\|x_r - x\|_{\mathcal{L}_1}^{[0, \tau]} < \rho_a,$$

where ρ_a is given in Eq. (25).

We now use Lemmas 4.1-4.2 to state the main result of the paper.

Theorem 4.1: Suppose that the stated assumptions and conditions in Eq. (27) hold. Consider a desired state trajectory $x^*(t)$ as in (3) and the state of the \mathcal{L}_1 closed-loop system defined via (1) and (8). Then we have

$$x(t) \in \Omega(\rho, x^*(t)), \quad \forall t \geq 0, \quad (32)$$

and the uniform ultimate bound, given by

$$x(t) \in \Omega(\delta(\omega, T), x^*(t)) \subset \Omega(\rho, x^*(t)), \quad \forall t \geq T > 0. \quad (33)$$

Here, the ultimate bound is defined as

$$\delta(\omega, T) := \mu(\omega, T) + \rho_a, \quad (34)$$

where the positive scalars ρ and ρ_a are defined in (25), and $\mu(\omega, T)$ is defined in Lemma 4.1.

A few critical comments are in order for the performance analysis. Let us first discuss the implication of the uniform bound ρ in Eq. (32). As per the definition in Eq. (25), $\rho = \rho_r + \rho_a$. It is evident from the definition that ρ is lower bounded by the initial condition difference $\|x_0^* - x_0\|$ and the positive scalars $\underline{\alpha}$ and $\bar{\alpha}$ which are associated with the CCM $M(x)$ of the nominal dynamics. Furthermore, as per the proof of Lemma 4.2, since $\rho_a \propto 1/\sqrt{\Gamma}$, the adaptation rate Γ can be increased to the maximum value allowable by the computation hardware to guarantee the smallest ρ_a , and thus, the smallest uniform bound ρ . However, the fact remains that the uniform bound ρ guaranteed by the \mathcal{L}_1 -controller for the tracking remains lower bounded by $\|x_0^* - x_0\|$. The only way this bound can be further reduced is if the underlying planner which provides the desired state-input pair $(x^*(t), u^*(t))$ can minimize $\|x_0^* - x_0\|$. Theorem 4.1 also provides the (uniform) ultimate bound

via $\delta(\omega, T)$ defined in Eq. (34). As already mentioned, $\rho_a \propto 1/\sqrt{\Gamma}$. Furthermore, from the definition of $\zeta_1(\omega)$ in Eq. (26a), it is evident that by choosing a large enough ω , there will always exist a known $0 < T < \infty$ such that $\delta(\omega, t) \leq \bar{\rho}$, for all $t \geq T$, for any chosen $\bar{\delta} > 0$. Therefore, we can always arbitrarily shrink the tube $\mathcal{O}(\bar{\delta})$ by choosing appropriate bandwidth ω and rate of adaptation Γ . This feature of the CCM-based \mathcal{L}_1 -controller is very advantageous, since, for example, this capability will allow the safe navigation of a robot through tight and cluttered environments. This improved performance, however, comes at the cost of reduced robustness that should be taken into consideration. The rate of adaptation Γ is obviously limited by the available computational hardware. More importantly, the role of the low-pass filter $C(s)$ in the \mathcal{L}_1 -control architecture (Fig. 2) is to decouple the control loop from the estimation loop [21]. Thus, increasing the bandwidth ω of $C(s)$ in order to get a tighter tube will lead to the $u_a(t)$ component of the \mathcal{L}_1 -input to behave as a high-gain signal, thus possibly sacrificing desired robustness levels [30]. Therefore, this trade-off must always be taken into account during the planning phase. Finally, it is important to note the semiglobal nature of the presented results, that for any arbitrarily large (but finite) tube width $\rho > 0$ and desired trajectory $x^*(t)$ in \mathcal{X}_ρ that the tube $\mathcal{O}(\rho)$ can be made invariant by appropriately selecting the adaptation rate and filter bandwidth.

V. CONCLUSIONS

We present a control methodology to enable safe feedback motion planning that relies on contraction theory and \mathcal{L}_1 -adaptive control. The proposed controller enables the a priori computation of uniform and ultimate-bounds which induce ‘tubes’ that can be taken into account by any planner of choice. In this way, the safety of the system is always guaranteed in the presence of uncertainties. Furthermore, by using the control law’s filter bandwidth and adaptation rate as tuning knobs, the width of the tubes can be adjusted arbitrarily as a trade-off between performance and robustness. The extended version of the paper with the preliminaries, simulation examples, and proofs can be found in [1].

REFERENCES

- [1] A. Lakshmanan, A. Gahlawat, and N. Hovakimyan, “Safe feedback motion planning: A contraction theory and \mathcal{L}_1 -adaptive control based approach,” *arXiv preprint arXiv:2004.01142*, 2020.
- [2] R. E. Mahony, V. Kumar, and P. I. Corke, “Multirotor aerial vehicles: Modeling, estimation, and control of quadrotor,” *IEEE Robotics & Automation Magazine*, vol. 19, pp. 20–32, 2012.
- [3] S. M. LaValle, *Planning algorithms*. Cambridge University Press, 2006.
- [4] R. Mahony and T. Hamel, “Robust trajectory tracking for a scale model autonomous helicopter,” *International Journal of Robust and Nonlinear Control: IFAC-Affiliated Journal*, vol. 14, no. 12, pp. 1035–1059, 2004.
- [5] S. Jeong and D. Chwa, “Coupled multiple sliding-mode control for robust trajectory tracking of hovercraft with external disturbances,” *IEEE Transactions on Industrial Electronics*, vol. 65, no. 5, pp. 4103–4113, 2017.
- [6] A. Donaire, J. G. Romero, and T. Perez, “Trajectory tracking passivity-based control for marine vehicles subject to disturbances,” *Journal of the Franklin Institute*, vol. 354, no. 5, pp. 2167–2182, 2017.
- [7] H. K. Khalil and J. W. Grizzle, *Nonlinear systems*. Prentice Hall Upper Saddle River, NJ, 2002, vol. 3.
- [8] L. Magni, H. Nijmeijer, and A. van der Schaft, “A receding-horizon approach to the nonlinear H_∞ control problem,” *Automatica*, vol. 37, pp. 429–435, 2001.
- [9] D. M. Raimondo, D. Limon, M. Lazar, L. Magni, and E. F. Camacho, “Min-max model predictive control of nonlinear systems: A unifying overview on stability,” *European Journal of Control*, vol. 15, no. 1, pp. 5–21, 2009.
- [10] X. Wang, L. Yang, Y. Sun, and K. Deng, “Adaptive model predictive control of nonlinear systems with state-dependent uncertainties,” *International Journal of Robust and Nonlinear Control*, vol. 27, no. 17, pp. 4138–4153, 2017.
- [11] S. V. Raković, “Set theoretic methods in model predictive control,” in *Nonlinear Model Predictive Control*. Springer, 2009, pp. 41–54.
- [12] S. V. Raković, W. S. Levine, and B. Aćıkmeşe, “Elastic tube model predictive control,” in *2016 American Control Conference (ACC)*. IEEE, 2016, pp. 3594–3599.
- [13] S. Yu, C. Böhm, H. Chen, and F. Allgöwer, “Robust model predictive control with disturbance invariant sets,” in *Proceedings of the 2010 American Control Conference*. IEEE, 2010, pp. 6262–6267.
- [14] G. Williams, B. Goldfain, P. Drews, K. Saigol, J. Rehg, and E. Theodorou, “Robust sampling based model predictive control with sparse objective information,” in *Proceedings of Robotics: Science and Systems*, June 2018.
- [15] B. T. Lopez, J. P. How, and J.-J. E. Slotine, “Dynamic tube MPC for nonlinear systems,” in *Proceedings of the 2019 American Control Conference*. IEEE, 2019, pp. 1655–1662.
- [16] I. R. Manchester and J.-J. E. Slotine, “Control contraction metrics: Convex and intrinsic criteria for nonlinear feedback design,” *IEEE Transactions on Automatic Control*, vol. 62, no. 6, pp. 3046–3053, 2017.
- [17] I. R. Manchester, J. Z. Tang, and J.-J. E. Slotine, “Unifying robot trajectory tracking with control contraction metrics,” in *Robotics Research*. Springer, 2018, pp. 403–418.
- [18] W. Lohmiller and J.-J. E. Slotine, “On contraction analysis for nonlinear systems,” *Automatica*, vol. 34, no. 6, pp. 683–696, 1998.
- [19] S. Singh, B. Landry, A. Majumdar, J.-J. Slotine, and M. Pavone, “Robust feedback motion planning via contraction theory,” *The International Journal of Robotics Research*, 2019, submitted.
- [20] B. T. Lopez and J.-J. E. Slotine, “Contraction metrics in adaptive nonlinear control,” *arXiv preprint arXiv:1912.13138*, 2019.
- [21] N. Hovakimyan and C. Cao, *\mathcal{L}_1 Adaptive Control Theory: Guaranteed Robustness with Fast Adaptation*. SIAM, 2010.
- [22] I. Gregory, E. Xargay, C. Cao, and N. Hovakimyan, “Flight test of an \mathcal{L}_1 adaptive controller on the NASA AirSTAR flight test vehicle,” in *Proceedings of AIAA Guidance, Navigation, and Control Conference*, Toronto, Ontario, Canada, August 2010, AIAA 2010-8015.
- [23] K. A. Ackerman, E. Xargay, R. Choe, N. Hovakimyan, M. C. Cotting, R. B. Jeffrey, M. P. Blackstun, T. P. Fulkerson, T. R. Lau, and S. S. Stephens, “Evaluation of an \mathcal{L}_1 adaptive flight control law on Calspan’s variable-stability Learjet,” *AIAA Journal of Guidance, Control, and Dynamics*, vol. 40, no. 4, pp. 1051–1060, 2017.
- [24] I. Kaminer, A. Pascoal, E. Xargay, N. Hovakimyan, C. Cao, and V. Dobrokhodov, “Path following for small unmanned aerial vehicles using \mathcal{L}_1 adaptive augmentation of commercial autopilots,” *AIAA Journal of Guidance, Control, and Dynamics*, vol. 33, no. 2, pp. 550–564, 2010.
- [25] H. Jafarnejadsani, D. Sun, H. Lee, and N. Hovakimyan, “Optimized \mathcal{L}_1 adaptive controller for trajectory tracking of an indoor quadrotor,” *AIAA Journal of Guidance, Control, and Dynamics*, vol. 40, no. 6, pp. 1415–1427, 2017.
- [26] X. Wang and N. Hovakimyan, “ \mathcal{L}_1 adaptive controller for nonlinear time-varying reference systems,” *Systems & Control Letters*, vol. 61, no. 4, pp. 455–463, 2012.
- [27] R. Schneider, *Convex Bodies: The Brunn-Minkowski Theory*. Cambridge University Press, 1993.
- [28] E. Lavretsky, T. E. Gibson, and A. M. Annaswamy, “Projection operator in adaptive systems,” *arXiv preprint arXiv:1112.4232*, 2011.
- [29] J.-B. Pomet and L. Praly, “Adaptive nonlinear regulation: Estimation from the Lyapunov equation,” *IEEE Transactions on Automatic Control*, vol. 37, no. 6, pp. 729–740, 1992.
- [30] C. Cao and N. Hovakimyan, “Stability margins of \mathcal{L}_1 adaptive control architecture,” *IEEE Transactions on Automatic Control*, vol. 55, no. 2, pp. 480–487, 2010.